01 Jan 1967

The Mechanism Of The Electrooxidation Of Acetylene On Gold

James W. Johnson
Missouri University of Science and Technology

J. L. Reed

William Joseph James
Missouri University of Science and Technology, wjames@mst.edu

Recommended Citation

J. W. Johnson et al., "The Mechanism Of The Electrooxidation Of Acetylene On Gold," *Journal of the Electrochemical Society*, vol. 114, no. 6, pp. 572 - 578, The Electrochemical Society, Jan 1967.
The definitive version is available at https://doi.org/10.1149/1.2426651

The Mechanism of the Electrooxidation of Acetylene on Gold

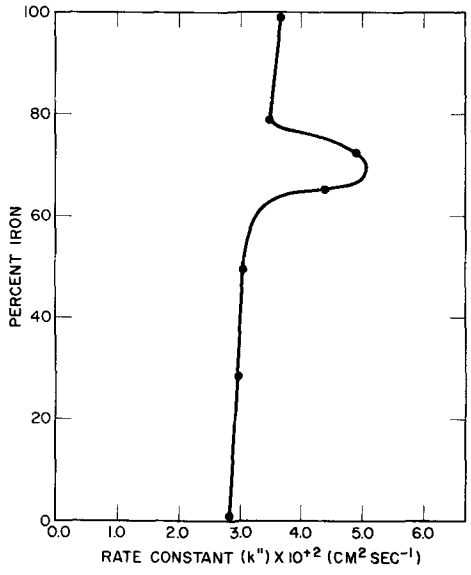

Fig. 10. Variation of rate constant with alloy composition

loy composition. There is a general decrease in the rate constant as the amount of iron in the alloy decreases except in the region between 65 to 75% iron. In this region, McKeehan (20) observed a change in crystal structure and noted a possible coexistence of the two structures and that either arrangement was on the verge on instability. It is of interest to note that on a plot of electrical resistance (of iron-nickel alloys) *vs.* percentage alloying element, there is a maximum in the curve at 30% nickel. This and several other anomalies in this region are ascribed to the fact that the iron-nickel alloys may be either ferrite, austenite, or both (21). An explanation for this increase in rate of penetration is that there are more grain boundaries in this region, and this presents an ease of penetration along these boundaries.

Summary

It has been shown that the experimental rate law for the absorption of hydrogen is

$$\text{Rate of absorption} = k[H_{ads}] + I$$

By controlling the current density it has been possible to obtain experimental conditions such that the rate law agreed with the following mechanism

$$H_{ads} \rightarrow H_{abs}$$

Studies of the effect of alloying iron with nickel show that the primary cause for changes in the rate of absorption of hydrogen is changes in the amount of adsorbed hydrogen.

Manuscript received Oct. 20, 1966; revised manuscript received March 13, 1967. This paper was presented at the Philadelphia Meeting, Oct. 9-14, 1966.

Any discussion of this paper will appear in a Discussion Section to be published in the December 1967 JOURNAL.

REFERENCES

1. T. C. Franklin and R. D. Sothern, *J. Phys. Chem.*, **58**, 951 (1954).
2. T. C. Franklin and S. L. Cooke, Jr., *This Journal*, **107**, 556 (1960).
3. T. C. Franklin and J. R. Goodwyn, *ibid.*, **109**, 288 (1962).
4. F. Matsuda and T. C. Franklin, *ibid.*, **112**, 767 (1965).
5. S. Schuldiner and T. P. Hoare, *Can. J. Chem.*, **37**, 228 (1959).
6. Z. Szklarska-Smialowska and M. Smialowski, *This Journal*, **110**, 444 (1963).
7. J. L. Weininger and M. Breiter, *ibid.*, **111**, 707 (1964).
8. M. A. V. Devanathan and M. Selvaratnam, *Trans. Faraday Soc.*, **56**, 1820 (1960).
9. C. N. Reilley, W. C. Cooke, and N. H. Furman, *Anal. Chem.*, **23**, 1031 (1951).
10. C. N. Reilley, W. C. Cooke, and N. H. Furman, *ibid.*, **24**, 1044 (1952).
11. C. C. Roth and H. Leidheiser, *This Journal*, **100**, 553 (1953).
12. W. D. Freitag, J. C. Mathias, and G. DiGuilio, *ibid.*, **111**, 35 (1964).
13. A. Eucken and B. Weblus, *Z. Elektrochem.*, **55**, 114 (1951).
14. M. Breiter, C. C. Knorr, and V. Volkl, *ibid.*, **59**, 681 (1955).
15. M. Breiter, H. Kammermaier, and C. A. Knorr, *ibid.*, **60**, 37 (1956).
16. M. Breiter, H. Kammermaier, and C. A. Knorr, *ibid.*, **60**, 119 (1956).
17. S. Schuldiner and R. M. Roe, *This Journal*, **110**, 332 (1963).
18. J. S. Ll. Leach and S. R. J. Saunders, **113**, 681 (1966).
19. T. C. Franklin, Unpublished work.
20. L. W. McKeehan, *Phys. Rev.*, **20**, 402 (1923).
21. J. W. Sands, "Metals Handbook," pp. 399-601, American Society for Metals, Novelty, Ohio (1948).

The Mechanism of the Electrooxidation of Acetylene on Gold

J. W. Johnson, J. L. Reed, and W. J. James

Departments of Chemical Engineering and Chemistry, The University of Missouri at Rolla, Missouri

ABSTRACT

Acetylene has been oxidized anodically in aqueous solutions at 80°C on gold electrodes. It was found that the partial oxidation to CO_2 was accompanied by a polymer formation. Effects of potential, acetylene partial pressure, pH, and temperature on the rate (current) were measured. A discontinuity in the Tafel curves was noted that indicated a change in the reaction mechanism with potential. The discontinuity was also pH dependent. A mechanism involving the discharge of H_2O and/or OH^- has been proposed that is consistent with the experimental results.

The electrooxidation of acetylene has been studied previously on platinized platinum electrodes (1). A reaction mechanism of the following sequence was proposed

$$C_2H_2\ (sol) \rightleftarrows C_2H_2\ (ads)$$
$$H_2O \rightleftarrows OH\ (ads) + H^+ + e$$
$$C_2H_2\ (ads) + OH\ (ads) \xrightarrow{\text{r.d.s.}} \ldots$$

The nature of the electrode is important in this mechanism as it is the source of oxygen-containing species (originating from water) for the oxidation reaction. The coverage of this species on platinum in the potential region where acetylene is oxidized is given by Dahms and Bockris as *ca.* 0.1. They also show the coverage on gold which is much smaller. This offers an indirect test of the mechanism in that it is an opportunity to observe the effect of decreasing the surface concentration of the oxygen containing species. In addition, the absence of electrons in gold for forming covalent bonds with adsorbed reactants and intermediates gives it important characteristics that deserve further study.

Experimental

Cell and apparatus.—The electrolytic cell was similar to that described previously (2, 3) unless otherwise stated. The working electrode (anode) was a rectangular piece of fine gold foil (0.005 in. thick) with a geometric area of 30.2 cm^2. The auxiliary electrode (cathode) was constructed of platinized platinum gauze. The procedure for activating the electrodes has been reported (2, 3). The reference electrodes were mercury-mercurous sulfate (1*N* H_2SO_4) for acid solutions and calomel (1*N* KCl) for basic solutions and were at 25°C during the experiments. All potentials of the gold anode are referred to the SHE as zero at the temperature of the experiment by means of the procedure described quantitatively below. All studies were made potentiostatically (except as noted) and at 80°C except for the activation energy determinations which ranged from 50° to 80°C.

Potential calculations.—The potentials listed in Table I were used in calculating the potentials of the gold anode. All, with the exception of those indicated with asterisks, were experimentally measured values. The measured potential differences between the gold anode and the reference electrodes were

$$\Delta V_{meas} = V - E_{ref,25}$$

In order that V might be referred to the SHE at the temperature of the experiment, the following relations were used

1. For the calomel (1*N* KCl) reference electrode

$$\begin{aligned} V &\equiv V - E_{H,t} \\ &= V - E_{C,25} - (E_{C,t} - E_{C,25}) + (E_{C,t} - E_{H,t}) \\ &= \Delta V_{meas} - (E_{C,t} - E_{C,25}) + (E_{C,t} - E_{H,t}) \end{aligned}$$

2. For the mercurous sulfate (1*N* H_2SO_4) reference electrode

$$\begin{aligned} V &\equiv V - E_{H,t} \\ &= V - E_{S,25} - (E_{S,t} - E_{S,25}) + (E_{S,t} - E_{C,t}) + (E_{C,t} - E_{H,t}) \\ &= \Delta V_{meas} - (E_{S,t} - E_{S,25}) + (E_{S,t} - E_{C,t}) + (E_{C,t} - E_{H,t}) \end{aligned}$$

Numerical values for terms shown in the parentheses were taken from Table I.

Reagents.—Sulfuric acid, sodium sulfate, sodium carbonate, and sodium hydroxide, "Fisher Certified" reagents; acetylene, Matheson purified (>99.6% purity); nitrogen, Matheson prepurified (>99.997% purity); and distilled water. Acetylene-nitrogen mixtures were made with the use of a dual-flow proportioner.

Coulombic efficiency.—The apparatus and procedure used to determine the coulombic efficiency in acidic solutions have been described previously (1). The cell was operated galvanostatically. In basic solutions, a gravimetric procedure was used in which the CO_2 absorbed in the 1*N* NaOH anolyte was precipitated as $BaCO_3$ by addition of barium acetate solution. The precipitate was collected, dried, weighed, and the CO_2 equivalent calculated. The exit gases from the cell were passed through a barium hydroxide absorber to insure that no CO_2 was escaping.

Table I. Data used for potential calculations

Electrodes	ΔE, v	Electrodes	ΔE, v
$E_{C,50} - E_{H,50}$	+0.2716*	$E_{C,50} - E_{C,25}$	+0.0125
$E_{C,60} - E_{H,60}$	+0.2672*	$E_{C,60} - E_{C,25}$	+0.0178
$E_{C,70} - E_{H,70}$	+0.2623*	$E_{C,70} - E_{C,25}$	+0.0230
$E_{C,80} - E_{H,80}$	+0.2567*	$E_{C,80} - E_{C,25}$	+0.0278
$E_{S,50} - E_{C,50}$	+0.362	$E_{S,50} - E_{S,25}$	+0.0063
$E_{S,60} - E_{C,60}$	+0.359	$E_{S,60} - E_{S,25}$	+0.0091
$E_{S,70} - E_{C,70}$	+0.357	$E_{S,70} - E_{S,25}$	+0.0117
$E_{S,80} - E_{C,80}$	+0.355	$E_{S,80} - E_{S,25}$	+0.0143

* Calculated from an expression given in Ives and Janz (9).
Subscripts. H, SHE; C, calomel (1*N* KCl) reference electrode; S, mercurous sulfate (1*N* H_2SO_4) reference electrode; numbers, t°C.

Results

Rest potentials.—Nitrogen was passed through the anodic and cathodic compartments for about 1 hr to remove oxygen from the cell. The flow through the anolyte was then replaced with acetylene or acetylene-nitrogen mixtures at a rate of 90 cm^3 (STP)/min. The values shown in Table II were obtained immediately on the admittance of acetylene and behaved similarly to those on platinum (1). The rest potentials varied very slightly in acidic solution, but the variation approached $\simeq$ —140 mv/pH unit in basic solutions. The rest potentials were independent of acetylene partial pressure.

Coulombic efficiency.—The results of the coulombic efficiency studies are shown in Table III.

After each test in acidic and neutral solutions, the anolyte was orange-brown in color, and the electrode had a thin, dark brown resinous film on it. The presence of the film had no noticeable effect on the current-potential relationships. At a constant potential, the current remained relatively constant (less than 10% change) for periods in excess of 24 hr, even though the film was forming. In 1*N* NaOH, the coloring of the electrolyte was present, but no film was formed on the electrode. Later experiments showed the film formed in the acidic electrolyte to be soluble in hot NaOH solutions, thus explaining its absence in the basic electrolyte.

By-product analysis.—Various tests and analyses were performed on the anolyte (both acidic and basic) and the resinous film from the acidic solutions in order to characterize the by-products.

1. The anolyte was extracted with ethyl ether, benzene, carbon tetrachloride, and n-hexane. Upon concentration of the extract, only the ether showed visible signs of any extracted material. An infrared spectrum of the extract indicated the presence of C=C and O—H bonds. A trace of the IR spectrum is shown in Fig. 1.

2. Negative results were obtained when the electrolyte was subjected to aldehyde and ketone tests,

Table II. Rest potentials for acetylene at 80°C

pH	V_{rest}, v (*vs.* SHE = 0 at 80°C)
0.35	+0.28
1.45	+0.28
6.0	+0.14
8.6	+0.03
11.6	−0.20
12.5	−0.34

Table III. Coulombic efficiency for CO_2 production for acetylene oxidation

Electrolyte	Acetylene pressure, atm	Efficiency, %
1*N* H_2SO_4	1.0	60 ± 5
	0.1	24
	0.01	3
1*N* NaOH	1.0	80 ± 10

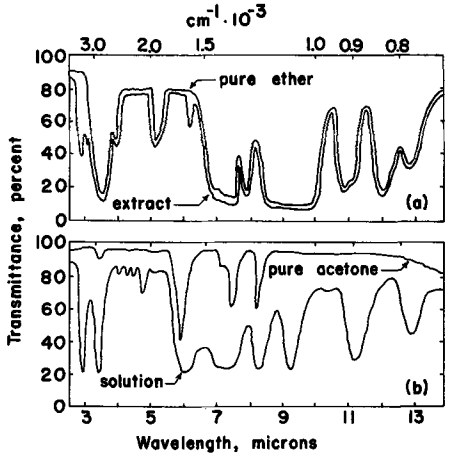

Fig. 1. Sketch of infrared spectra of (a) ether extract of acidic anolyte and (b) concentrated solution of resin dissolved in acetone.

indicating an absence of CHO and C=O groups in the by-products.

3. The resinous material was subjected to solvation tests in the solvents mentioned above plus acetone, methanol, 2*N* H_2SO_4, and 2*N* NaOH. Only in hot NaOH did the resin dissolve readily. Concentration of the acetone and methanol solvents showed visible signs of dissolved material. An infrared spectrum of the acetone solution confirmed the O—H bond and indicated a C—O bond, possibly a C—OH bond (see Fig. 1). An emulsion of the resin was also prepared with fluorlube, but IR analysis was unsuccessful.

4. A carbon-hydrogen-oxygen analysis[1] of the resinous film gave a C:H:O atomic ratio of approximately 2:2:1.

The most likely structures of the by-product that are consistent with the analyses are an unsaturated polyhydroxyl compound and a mixed hydroxyl structure with ether linkages. Any structure of the latter type with the proper C:H:O ratio contains an unconjugated enol form which has doubtful stability with respect to a keto shift. Thus, it seems that the most probable structure is of the type, —C(H)=C(OH)—C(H)=C(OH)—. A poly-hydroxyl structure of this type would be stable due to the conjugated bonding. It would also behave chemically similar to a phenol which accounts for its solubility in strong base.

Analysis of the exit gases from the electrolysis cell showed that no volatile, partially oxidized hydrocarbons were present. Hence, it was assumed that the only by-product was the polyhydroxyl compound at various degrees of polymerization.

Current-potential relation.—Tafel curves are shown in Fig. 2. The current values at a constant potential could be reproduced within 5%. There seems to be a transition region (discontinuity) in the plots for *p*H values of six and greater. This region is shifted upward along the Tafel curve as the *p*H is increased. The slope of the Tafel curve, both above and below the transition region, is approximately 140 mv. The increasing slope at the upper end of the curves is assumed to be due to either passivation phenomena or ohmic drop in the reference circuit. The time effects were essentially the same as those for the oxidation of acetylene on platinum (1). However, unlike platinum, no potential region of complete passivation was found for the gold electrode below oxygen evolution.

*p*H *effect.*—The effect of *p*H at constant ionic strength is also shown in Fig. 2. Qualitatively, in strong acids, $\partial \log i/\partial pH \simeq 0$. This value increased with *p*H, reaching unity in basic solutions.

[1] Analysis performed by Galbraith Laboratories, Knoxville, Tennessee.

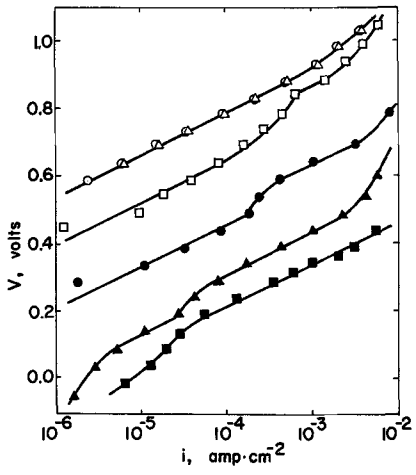

Fig. 2. Current-potential relation (P_A = 1 atm) as a function of *p*H at 80°C. (○, *p*H = 0.35; △, 1.45; □, 6.0; ●, 8.6; ▲, 11.6; ■, 12.5) (Potentials *vs.* SHE = 0 at 80°C).

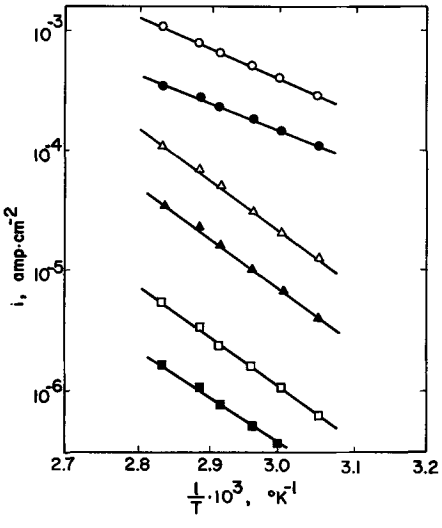

Fig. 3. Current-temperature relation (P_A = 1 atm) as a function of potential. (○, 0.368v, 1N NaOH; ●, 0.318v, 1N NaOH; △, 0.832v, 1N H_2SO_4; ▲, 0.732v, 1N H_2SO_4; □, 0.018v, 1N NaOH; ■, —0.032v, 1N NaOH; ○, ●, □, ■, below transition region; △, ▲, above transition region) (Potentials *vs.* SHE = 0 at temperature of experiment).

Temperature effect.—The effect of temperature on current in 1*N* H_2SO_4 and 1*N* NaOH (above and below the transition region) is shown in Fig. 3. Activation energies were calculated and are shown in Table IV.

Values of $\partial(E_a)/\partial V$ are approximately equal to αF = —11.5 kcal/v for α = 0.5. In 1*N* NaOH, it should be noted that the potential change does not account for the entire difference between activation energies above and below the transition region. This suggests that some change or alteration may have been made in

Table IV. Activation energies for the anodic oxidation of acetylene on gold electrodes

Electrolyte	Potential, v (*vs.*SHE = 0 at temperature of experiment)	Activation energy, kcal at SHE potential	$\partial(E_a)/\partial V$, kcal/v
1*N* H_2SO_4	0.732	19.9	—11.9
	0.832	18.8	
1*N* NaOH	0.368*	12.6	—12.0
	0.318*	13.2	
	0.018**	18.7	—12.0
	—0.032**	19.3	

* Above the transition region.
** Below the transition region.

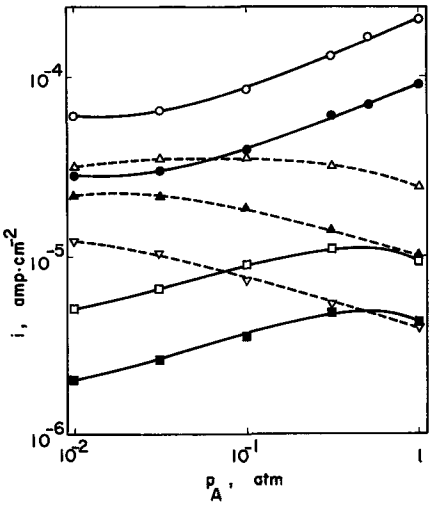

Fig. 4. Current-acetylene partial pressure relation as a function of potential at 80°C. (○, 0.268v, 1N NaOH; ●, 0.218v, 1N NaOH; □, 0.068v, 1N NaOH; ■, 0.018v, 1N NaOH; △, 0.732v, 1N H_2SO_4; ▲, 0.682v, 1N H_2SO_4; ▽, 0.632v, 1N H_2SO_4, △, ▲, ▽, □, ■, below transition region; ○, ●, above transition region.) (Potentials vs. SHE = 0 at 80°C).

the reaction mechanism. Due to mixed reactions, the reversible potential could not be evaluated in order to calculate the true (chemical) activation energy.

Pressure effect.—Partial pressure studies were made in 1*N* H_2SO_4 and 1*N* NaOH. The results are shown in Fig. 4. In 1*N* H_2SO_4, the pressure effect ($\partial i/\partial p$) was negative. In 1*N* NaOH below the transition region, the pressure effect started out negative, then became positive at pressures <0.1 atm. In 1*N* NaOH above the transition region, the effect was positive at pressures >0.1 atm and approached a constant value at pressures <0.1 atm. Under the latter conditions (1*N* NaOH, above transition region), appreciable residual currents were noted when the acetylene flow was stopped after several minutes of electrolysis. Other measurements made in fresh electrolyte showed the pressure effect to be positive over the entire range, 0.01 to 1 atm. However, due both to the residual currents and the smallness of the values, it was felt that only measurements above 0.1 atm were of sufficient accuracy to be considered valid for pressure-current correlations.

Discussion

Adsorption of Acetylene

The adsorption of acetylene on Pt has been discussed in the previously mentioned paper (1). The isotherm (Langmuir) was formulated as

$$\frac{\theta_A}{(1-\theta_A)^4} = K_p P_A$$

where θ_A is the fractional coverage by acetylene, p_A is the acetylene partial pressure, and K_p is the adsorption constant for the isotherm relating coverage to partial pressure. The order of magnitude of K_p, estimated both by an indirect method and correlation of experimental data, was 10^4-10^6 atm^{-1}. No data are available which would allow an independent evaluation of K_p for acetylene adsorption on Au from solution.

The most probable attachment of acetylene to a metal surface is (4)

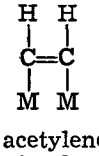

There is evidence that acetylene forms covalent bonds with the metal surface in the case of Pt and Au by rearrangement to dsp hybrids (4, 5). Platinum has 0.5 vacant d-orbitals per atom available for covalent bonding, thus acetylene was assumed to have a 4 site attachment (1). Gold has no statistically calculated d-orbitals available for covalent bonding (6), therefore the number of sites occupied (covered) will be ascertained from a scaled diagram of an acetylene molecule adsorbed on a gold surface (Fig. 5). The acetylene covers only two sites, but possibly blocks two others due to its size. Therefore, the isotherm for the adsorption of acetylene on Au is taken as

$$\frac{\theta_A}{(1-\theta_A)^n} = K_p P_A \qquad [1]$$

where n can be equal to 2 or more.

Reaction Mechanism

The rate-determining step below the transition region must exhibit the following characteristics: (*i*) Be the first electron transfer since the Tafel slope is $2(2.3\ RT/F)$, (*ii*) involve a species other than adsorbed acetylene, (or derived therefrom) since $\partial i/\partial p < 0$, and (*iii*) exhibit essentially no *p*H dependence in strong acid solutions but show a dependency, $\partial \log i/\partial p\text{H} \simeq 1$ in strong base solutions.

Above the transition region, the rate-determining step must: (*i*) again be the first electron transfer since the Tafel slope remains $2(2.3\ RT/F)$, (*ii*) involve adsorbed acetylene (or a species derived therefrom) since $\partial i/\partial p > 0$, and (iii) exhibit a *p*H dependence $\partial \log i/\partial\ p\text{H} \simeq 1$ in going from weak acid to strong base solutions.

There is apparently competition (branching reactions) between intermediates species in regard to the formation of the resin material and total oxidation products, CO_2 and H^+ (or H_2O). As the faradaic efficiency was not greatly affected by potential or *p*H, this competition probably occurs after the r.d.s. in the different regions. The effect of acetylene partial pressure on the efficiency will be discussed later.

Below the transition region (b.t.r.), the substances involved in the r.d.s. must be OH^- or H_2O. This is as proposed previously as a source of OH radicals involved in the oxidation of acetylene and ethylene on Pt (1-3). Currents depending on the discharge of OH^- would be diffusion limited up to *p*H's of 6 to 8 at the current densities used in this study. Thus, the reaction sequence can be represented as

$$C_2H_2 \rightleftarrows C_2H_2\ (\text{ads}) \qquad [2]$$

$$\left.\begin{aligned} H_2O &\rightarrow OH\ (\text{ads}) + H^+ + e \\ OH^- &\rightarrow OH\ (\text{ads}) + e \end{aligned}\right\}\ \text{r.d.s.} \qquad [3a],\ [3b]$$

$$C_2H_2\ (\text{ads}) + OH\ (\text{ads}) \rightarrow \ldots$$

$$\rightarrow CO_2 + H^+ + \text{electrons} + \text{resin} \qquad [4]$$

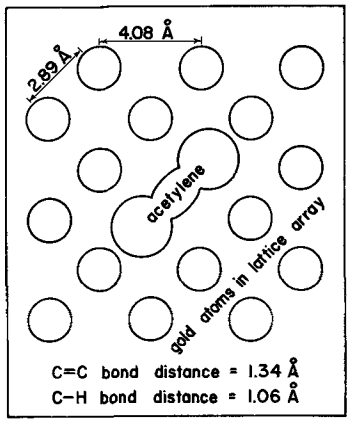

Fig. 5. Schematic diagram of an acetylene molecule adsorbed on a gold surface.

The anodic oxidation of acetylene can be expressed as

$$i_{b.t.r.} = n\mathbf{F}(k_{3a}a_{H_2O} + k_{3b}a_{OH^-})(i - \theta_T)\exp(\alpha\mathbf{F}V/RT) \quad [5]$$

where k_{3a} is the rate constant for water discharge and k_{3b} is the rate constant for OH^- discharge. The coverage of OH radicals is very low (6), and the coverage of all other intermediates can be neglected in comparison with θ_A since they occur in the reaction sequence after the r.d.s. Thus, $\theta_T \simeq \theta_A$, and

$$i_{b.t.r.} = n\mathbf{F}(k_{3a}a_{H_2O} + k_{3b}a_{OH^-})(1 - \theta_A)\exp(\alpha\mathbf{F}V/RT) \quad [6]$$

Above the transition region (a.t.r.), the r.d.s. involves either adsorbed acetylene or a radical derived therefrom. The dissociative adsorption of acetylene can be disregarded due to previous considerations of the energy involved (1) and to the pH effect observed in this study. The studies on Pt (1) also indicated there was no hydrolysis of acetylene in solution. A reaction sequence that meets all the requirements is

$$C_2H_2 \rightleftarrows C_2H_2\,(ads) \quad [7]$$

$$\left.\begin{aligned} C_2H_2(ads) + H_2O &\rightarrow C_2H_2OH(ads) + H^+ + e \quad [8a] \\ C_2H_2(ads) + OH^- &\rightarrow C_2H_2OH(ads) + e \quad [8b] \end{aligned}\right\}\text{r.d.s.}$$

This gives the anodic oxidation rate as

$$i_{a.t.r.} = n\mathbf{F}(k_{8a}a_{H_2O} + k_{8b}a_{OH^-})\,\theta_A \exp(\alpha\mathbf{F}V/RT) \quad [9]$$

pH dependence.—Current-pH values were calculated from Eq. [6], representing rates below the transition region, considering the term $[n\mathbf{F}(1 - \theta_A)\exp(\alpha\mathbf{F}V/RT)]$ constant at a given potential over the entire pH range. The contribution of $k_{3a}a_{H_2O}$ was calculated from an experimental value of the current in 1*N* H_2SO_4. Here the contribution from OH^- discharge would be negligible due to its low concentration. The contribution of $k_{3b}a_{OH^-}$ was calculated in 1*N* NaOH assuming $k_{3a}a_{H_2O}$ to be insignificant. Experimentally this is justified as the $\partial \log i/\partial$ pH $\simeq 1$ in strong base. It was necessary to make a correction for the electrolyte pH at the electrode-solution interface due to the diffusion, away from the electrode, of H^+ produced by the reaction. This correction was significant only for bulk electrolyte pH's in the range 5 to 9. Using these constants, the pH dependence from Eq. [6] over the entire pH range is shown in Fig. 6. The experimental data are also included for comparison. Above the transition region, where Eq. [9] applies, it was not possible to consider the contribution of $k_{8a}a_{H_2O}$ as experimental data were available only for pH's > 6. Evaluating $k_8a_{OH^-}$ in a similar manner as described above gives the pH-current relationship also shown in Fig. 6. It can be seen that Eq. [6] and [9] correlate these experimental data in their respective regions.

Partial pressure dependence.—Qualitatively, the rate dependence on acetylene partial pressure can be summarized as follows. (*A*) acid solution (below transition region), $\partial i/\partial p < 0$, Eq. [6] applies. (*B*) Base solutions (above transition region), $\partial i/\partial p > 0$, Eq. [9] applies. (*C*) Base solution (below transition region), for $p > 0.5$ atm, $\partial i/\partial p < 0$, and for $p < 0.5$ atm, $\partial i/\partial p > 0$, *i.e.*, Eq. [6] applies at higher pressures while Eq. [9] applies at the lower ones.

The data from acid solutions (b.t.r.) were correlated using Eq. [6] for which the acetylene coverage was calculated from Eq. [1] with assumed values of n and K_p as 4 and 10^4, respectively. The procedure for these calculations has been described (1). The predicted values as well as experimental data are shown in Fig. 7.

A similar treatment of data from base solution (a.t.r.) using Eq. [1] and [9] is also shown in Fig. 7. Here, values of n and K_p were 8 and 2.5, respectively. It should also be pointed out that $n = 4$ and $K_p = 3.5$ correlated the data within experimental errors, although not as well as the first-mentioned values. These pressure effects can be related to a reaction mechanism if it is assumed that the amount of acetylene adsorbed onto gold decreases as the pH of the solution increases, and H_2O (or OH^-) will undergo discharge only when adsorbed adjacent to an adsorbed acetylene molecule. The first assumption is consistent with trends noted for the adsorption of some other organic compounds from solution (7). Since the oxide (hydroxide) coverage on gold is very low at these potentials in the absence of adsorbed acetylene (6), then H_2O (or OH^-) discharge does not occur readily. Thus, the second assumption could be considered feasible. With these assumptions, the coverages of acetylene on gold can be pictured as shown in Fig. 8a and 8b. In the first case (Fig. 8a) for high coverage, it can be seen that most any adsorption site available for H_2O (or OH^-) will be adjacent to an adsorbed acetylene molecule; thus H_2O (or OH^-) will be discharged and the rate will be proportional to $(1 - \theta_A)$. If due to geometric considerations, four adjacent vacant sites were necessary

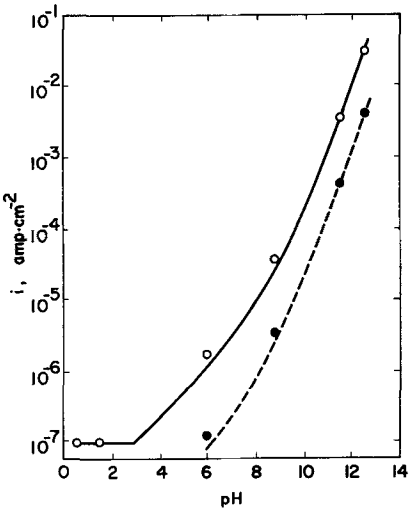

Fig. 6. Theoretical current pH relation at constant potential = 0.40v. (—, Eq. [6]; ○, experimental data below transition region; - -, Eq. [9]; ●, experimental data above transition region).

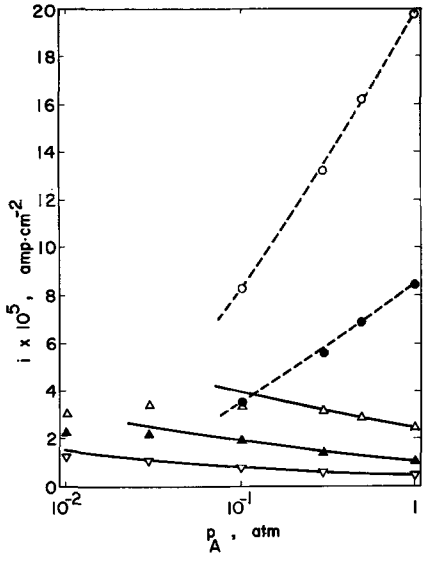

Fig. 7. Theoretical current-acetylene partial pressure relation as a function of potential at 80°C. (○, 0.268v, 1N NaOH; ●, 0.218v, 1N NaOH; - -, Eq. [9], data above transition region; △, 0.732v, 1N H_2SO_4; ▲, 0.682v, 1N H_2SO_4; ▽, 0.632v, 1N H_2SO_4; —, Eq. [6], data below transition region) (Potentials vs. SHE = 0 at 80°C).

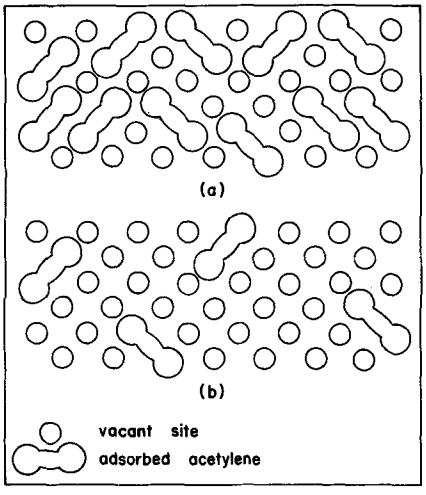

Fig. 8. Schematic diagram of acetylene molecules adsorbed on a gold surface at (a) high and (b) low coverage.

for the acetylene to adsorb, then this model would be consistent with the values of $n = 4$ and $K_p = 10^4$. In the second case (Fig. 8b) for low coverage, there are considerable available sites for water (or OH^-) to adsorb that are not adjacent to adsorbed acetylene molecules. Discharge does not occur on these sites, therefore, the rate is proportional to θ_A rather than $(1 - \theta_A)$. This case is consistent with the lower value of K_p (equal to 2.5). The higher value of n can also be rationalized to some extent if one considers that, for reaction to take place, acetylene must adsorb on a spot that has more than four adjacent vacant sites so that the discharge of water can be accommodated.

Acetylene coverages have been calculated for Eq. [6] and [9] and are shown in Table V. These coverages are also such that Langmuir-type adsorption is approximated.

In base solutions (b.t.r.) where the pressure dependence changes from negative to positive, *i.e.*, the expression for the current changes from Eq. [6] to Eq. [9], there would necessarily have to be a higher acetylene coverage than in base solutions above the transition region. This would suggest the acetylene coverage may have some potential as well as pH dependence.

Reaction products.—The most probable explanation for the incomplete oxidation of acetylene on a gold electrode is similar to that suggested by Dahms and Bockris pertaining to the anodic oxidation of ethylene on various rare metals (6). Using Pauling's equation (8) for the strength of a covalent bond between a metal and a carbon atom, it can be shown that the Au-C bond is about 45 kcal less than the Pt-C bond. Thus, a partially oxidized intermediate could break away from an Au surface before being completely oxidized much easier than from a Pt surface. Due to the reactiveness of the partially oxidized compounds (possibly radicals) and acetylene, polymerization products would be expected.

Summary

The anodic oxidation of acetylene has been studied at 80°C in solutions of H_2SO_4, Na_2SO_4, and NaOH of constant ionic strength. The reaction rate was determined as a function of potential, pH, acetylene partial pressure, and temperature. Coulombic efficiencies were determined for CO_2 production in both acidic and basic solutions. Two regions of linear Tafel behavior separated by a transition region were found.

The following kinetic parameters were noted:

Below the transition region

$$\frac{\partial V}{\partial \log i} = 140 \text{ mv}, \frac{\partial i}{\partial p} < 0$$

$$\frac{\partial \log i}{\partial \text{ pH}} = 1 \text{ (weakly acidic and basic solutions)}$$

Above the transition region

$$\frac{\partial V}{\partial \log i} = 140 \text{ mv}, \frac{\partial i}{\partial p} > 0$$

$$\frac{\partial \log i}{\partial \text{ pH}} = 0 \text{ (moderate to strong acid solutions)}$$

$$\frac{\partial \log i}{\partial \text{ pH}} = 1 \text{ (weakly acidic and basic solutions)}$$

The acetylene was partially oxidized to CO_2 with some polymer formation. The coulombic efficiency for CO_2 production was 60 ± 5% in acidic and 80 ± 10% in basic solutions and decreased with decreasing acetylene partial pressure. The most probable structure of the polymer was $-\overset{H}{\underset{|}{C}}=\overset{OH}{\underset{|}{C}}-\overset{H}{\underset{|}{C}}=\overset{OH}{\underset{|}{C}}-$. Activation energies in the linear Tafel regions varied from 12-20 kcal. The potential dependence of the activation energy, $\partial E_a/\partial V$, was −12 kcal/v.

The reaction mechanisms in the linear Tafel regions were interpreted in terms of the following sequences.

Below the transition region

$$C_2H_2 \rightleftarrows C_2H_2 \text{ (ads)}$$

$$\left.\begin{aligned} &H_2O \rightarrow OH \text{ (ads)} + H^+ + e \\ &OH^- \rightarrow OH \text{ (ads)} + e \end{aligned}\right\} \text{r.d.s.}$$

$$C_2H_2 \text{ (ads)} + OH \text{ (ads)} \rightarrow \ldots$$

Above the transition region

$$C_2H_2 \rightleftarrows C_2H_2 \text{ (ads)}$$

$$\left.\begin{aligned} &C_2H_2 \text{ (ads)} + H_2O \rightarrow C_2H_2OH \text{ (ads)} + H^+ + e \\ &C_2H_2 \text{ (ads)} + OH^- \rightarrow C_2H_2OH \text{ (ads)} + e \end{aligned}\right\} \text{r.d.s.}$$

The discharge of H_2O and/or OH^- was necessary to explain the observed pH effect.

Table V. Calculated pressure-coverage relationships for the adsorption of acetylene on gold electrodes at 80°C

Eq. [6] ($K_p = 10^4$, $n = 4$) P_A (atm)	θ_A	Eq. [9] ($K_p = 2.5$, $n = 8$) P_A (atm)	θ_A
1.0	0.90	1.0	0.25
0.3	0.87	0.5	0.20
0.1	0.83	0.3	0.17
0.03	0.78	0.2	0.14
0.01	0.72	0.1	0.10

Acknowledgments

The authors wish to thank the National Aeronautics and Space Administration for a traineeship which one of the authors (J.L.R.) held during the course of this investigation. Thanks are also due to Dr. S. B. Hanna of the Chemistry Department for helpful discussions. This paper is based on a dissertation presented by one of the authors (J.R.L.) in partial fulfillment of the degree, Doctor of Philosophy, at the University of Missouri at Rolla.

Manuscript received Aug. 12, 1966; revised manuscript received March 3, 1967. This is paper No. 16 from the Graduate Center for Materials Research of the Space Sciences Research Center at Rolla.

Any discussion of this paper will appear in a Discussion Section to be published in the December 1967 JOURNAL.

REFERENCES

1. J. W. Johnson, H. Wroblowa, and J. O'M. Bockris, *This Journal*, **111**, 863 (1964).
2. M. Green, J. Weber, and V. Drazic, *ibid.*, **111**, 721 (1964).
3. B. Piersma, H. Wroblowa, and J. O'M. Bockris, *J. Electroanalyt. Chem.*, **6**, 401 (1963).
4. B. M. V. Trapnell, "Chemisorption," Butterworths, London (1955).
5. G. C. Bond, "Catalysis by Metals," Academic Press, London, New York (1962).
6. H. Dahms and J. O'M. Bockris, *This Journal*, **111**, 728 (1964).
7. J. O'M. Bockris, D. Swinkels, and M. Green, *Rev. Sci. Instr.*, **33**, 18 (1962).
8. L. Pauling, "The Nature of the Chemical Bond," Cornell University Press, Ithaca, N. Y. (1960).
9. D. J. G. Ives and G. J. Janz, "Reference Electrodes," Academic Press, London, New York (1961).

The Thermal Temperature Coefficient of the Calomel Electrode Potential between 0° and 70°C

I. Experimental Results in Aqueous Potassium, Sodium, Lithium, Calcium Chlorides and in Hydrochloric Acid

Andre J. de Bethune, Henry O. Daley, Jr., Nancy A. Swendeman Loud, and G. Robert Salvi

Laboratory of Physical and Nuclear Chemistry, Boston College, Chestnut Hill, Massachusetts

ABSTRACT

The initial thermal temperature coefficient of the calomel electrode potential has been measured between 0° and 70°C for aqueous 1.0, 0.1, and 0.01*m* potassium chloride, sodium chloride, lithium chloride, hydrochloric acid and 0.5, 0.05, and 0.01*m* calcium chloride. Thermal diffusion of the electrolyte was impeded by the use of Vycor intermediate (thirsty glass) glass plugs in the salt bridges between the two banks of electrodes, one of which was kept at 35° while the other was varied from 0° to 70°. The thermal emfs of the fifteen cells investigated exhibited a slight curvature concave to the temperature axis. The hot electrode had the (+) polarity (cathodic in a battery sense) in all cases. Experimental data can be fairly represented by quadratic equations, and least squares values of the quadratic constants are given. The initial thermal temperature coefficients are compared with prior thermal emf data on the calomel electrode. The relative thermal emfs of the same electrode in different salts at constant chloride ion concentration are compared with values deduced from prior thermal emf observations on calomel and silver chloride electrodes or calculated from the transport entropies of chlorides obtained in thermal diffusion studies.

The thermal temperature coefficient $(dV/dT)_{th}$ of the potential of an electrode is the temperature derivative of dE/dT_2 of the initial emf (*i.e.*, before thermal diffusion sets in) $E = V'' - V'$ of the thermal cell

$$\mathrm{Cu}(T_1,V')/\mathrm{Electrode}(T_1)/\mathrm{Electrolyte}(T_1)/\mathrm{Electrolyte}(T_2)/\mathrm{Electrode}(T_2)/\mathrm{Cu}(T_2)/\mathrm{Cu}(T_1,V'') \quad [1]$$

in which the temperature T_1 is fixed and T_2 varies. The thermal temperature coefficient is given a positive value when the hot electrode is the (+) or cathodic terminal of the thermal cell, as is the case experimentally with all calomel electrodes studied.

The thermal temperature coefficient of the calomel electrode potential was originally studied by Gockel (1) and later in more detail by Richards (2). Subsequent investigations were conducted by Fales and Mudge (3), Ewing (4), Sorensen and Linderstrom-Lang (5), Kolthoff and Tekelenburg (6), Bjerrum and Unmack (7), Burian (8), Young (9), Wingfield and Acree (10), Cary and Baxter (11), and Ikeda and Kimura (12) (who investigated only differences between temperature coefficients in various aqueous chlorides). In most thermal emf studies, the temperature differential has been kept between 5° and 10°C, and the thermal temperature coefficient assumed to be valid at the median temperature, which was usually between 15° and 25°C.

Thermal emf data (13, 14) can be used to determine relative values of the entropies of diffusion transport S^D (Soret transport entropies), and of the conjugate heats of transfer Q^*, of electrolytes. They can also throw light on the several ionic transport entropies, *viz.*, the ionic entropy of electrochemical transport S^{E}_i (the so-called "absolute" partial molal entropy of an ion), and the ionic entropy of migration transport S^{M}_i [the entropy of transfer, Eastman's entropy, in Agar's (15) terminology], with its conjugate ionic heat of transfer Q^*_i, as well as the sum of the two ionic transport entropies $\bar{\bar{S}}$ $(= S^{E}_i + S^{M}_i)$ introduced by Temkin and Khoroshin (16) as the entropy of the moving ion, and referred to by Agar (15) as the transported entropy of the ion. Because of the intrinsic interest of thermal emfs as an experimental source of information for these transport entropies of electrolytes and ions, the thermal temperature coefficient of the calomel electrode was reexamined in the present investigation by measuring the thermal emf between banks of half-cells at 35°C, and at a variable temperature t ranging from 0° to 70°C, for three levels of concentration of five different aqueous chloride electrolytes.

Experimental

The thermal emf of the calomel electrode was determined for the following electrolytes: potassium chloride, sodium chloride, lithium chloride, and hydrochloric acid at 25°C concentrations of 1.0, 0.10, and 0.01 moles per liter, and calcium chloride at 25°C concentrations of 0.50, 0.05, and 0.01 moles per liter. The salts and acid used were of reagent grade. The sodium, potassium, and lithium salts were dried at 110°C and the solutions prepared by dilution of the weighed dried salt in a volumetric flask. Hydrochloric acid solutions were prepared directly by dilution of stock concen-